π-Complexation for olefin/paraffin separation using aluminosilicates

A. Luna-Triguero, A. Slawek, R. Sánchez-De-Armas, J.J. Gutiérrez-Sevillano, C.O. Ania, J.B. Parra, J.M. Vicent-Luna, S. Calero

Luna-Triguero A, Sławekb A, Sánchez-de-Armas R, Gutiérrez-Sevillano JJ, Ania CO, Parra JB, Vicent-Luna JM, Calero S. pi-complexation for olefin/paraffin sparation using Aluminosilicates, Chemical Eng. J 380 (2020) 122482.

10.1016/j.cej.2019.122482

hal-02351368v1

π-complexation for olefin/paraffin sparation using Aluminosilicates

A. Luna-Triguero[a], A. Sławek[b], R. Sánchez-de-Armas[c], J. J. Gutiérrez-Sevillano[a], C. O. Ania[d], J. B. Parra[e], J. M. Vicent-Luna[a]*, and S. Calero[a]*

[a]Department of Physical, Chemical and Natural Systems, Universidad Pablo de Olavide, Ctra. Utrera Km. Seville ES-41013, Spain

[b] Faculty of Chemistry, Jagiellonian University, Gronostajowa 2, 30-387 Kraków, Poland

[c] Departamento de Química Física, Universidad de Sevilla, Seville ES-41012, Spain

[d] CEMHTI (UPR 3079), CNRS, Univ. Orléans, 45071 Orléans, France

[e] Instituto Nacional del Carbón (INCAR, CSIC), Oviedo, Spain

Corresponding authors:
Email: jmviclun@upo.es
Email: scalero@upo.es

Abstract

The purification of the α-olefins though challenging, is mandatory step for their use in the chemical industry. Since adsorptive separation using zeolites is one of the most promising alternatives for olefin/paraffin separation in terms of energy efficiency, we use a combination of experiments and molecular simulations to study the effect that the topology and chemical composition of the zeolite exert on the purification of olefins. To this aim we developed an effective potential for the cations with the double bond of the olefins. The potential parameters were validated with our experimental adsorption isotherms and isobars of propylene and 1-hexene. We performed an extensive study of propane/propylene separation in more than 200 all silica zeolites and several aluminosilicates. We also performed DFT and classical optimization of the structures which is key factor for the adsorption mechanisms. DFT calculations also allowed the analysis of binding energies and binding geometries of propane and propylene in NaY and LTA5A. We discussed the effect exerted by the cations on the separation performance of the zeolites. Our study shows that aluminosilicates with calcium cations are the best candidates to separate olefins from paraffins, due to the stronger interaction of the double bond of olefins with these divalent cations.

Introduction

Linear α-olefins are widely used in industry. Propylene is an important light olefin used in refinery operations. It is a petrochemical raw material used in rubber and plastic industries, and as intermediate compound for the production of polypropylene. The propylene demand is growing due to the increment of polypropylene production.[1] However, the production of propylene is limited.[2] Larger α-olefins with chain length from four to eight carbon atoms (C4-C8) are used for production of aldehydes *via* oxo synthesis to produce short fatty acids.[2] 1-butene, 1-hexene and 1-octene are used as comonomers in the manufacture of high-density polyethylene (HDPE) and linear low-density polyethylene (LLDPE).[3] Light olefins are obtained primarily by stream cracking or as a product of fluid catalytic cracking of gas oils in refineries. In order to obtain the polymer-grade olefin, the separation of olefin from paraffin is required. This separation is a challenging procedure that is conventionally achieved by distillation, which is energy-intensive and has a high operational cost due to the close boiling point of the compounds.[4] Among several new energy-efficient alternatives, adsorptive separation is one of the most promising techniques.[5] While cryogenic distillation relies on small differences in the boiling points of olefin and paraffin components, adsorptive separations take advantage of dissimilar physical properties such as kinetic diameters, polarity, and polarizability of the adsorbates. In this regard, the selection of adsorbents with optimal selectivity and adsorption capacity is an important step when designing the whole adsorption process. Zeolites have been extensively studied for olefin/paraffin separation. Pure silica zeolites rarely achieve great separations except for kinetic separation in some zeolites, for instance ITQ-12.[6-8] Sodium and calcium forms of zeolite X were studied via gas chromatographic methods to determine the potential separation of ethylene from ethane and methane,[9] and a large variety of 13X zeolites[10-12] including Li^+, K^+, Rb^+, and Cs^+ cation exchanged forms have been proposed for olefin/paraffin separation.[13-14] There are many experimental studies on the adsorption of olefin and paraffin in zeolites LTA4A and LTA5A. These zeolites have also been proposed as adsorbent for some targeted separations.[15-17]

There are a large number of zeolites covering a wide range of topologies and chemical composition. This makes difficult the search of an efficient adsorbent for a given process. In this sense, molecular simulation is an efficient tool to predict physical and chemical properties of materials. The accuracy of classical simulations depends on the models and force fields used to describe the systems. Experimental data are in most cases crucially important for validation of the force fields used in simulation. The use of molecular simulations for adsoption isotherms of paraffins in pure silica zeolites is being reported in many works.[8, 18-20] Most of these works use the force field developed for Dubbeldam et al.,[21] that is accurate and can reproduce experimental data for pure silica zeolites. However, olefins have not been extensively studied using molecular simulation for being more complex. In these molecules, electrostatic interactions play an important role, particularly in aluminosilicates. In this work we propose a set of Lennard-Jones parameters to model the interaction of cations (Na^+ and Ca^{2+}) with the double bond of olefins. This is essential contribution by itself since (1) molecular simulation studies in aluminosilicate zeolites for olefin/paraffin separation are scarce and (2) available parameters are reported for a given structures and not transferable to other topologies.[17, 22-23] In this regard, we developed a transferable set of parameters to reproduce the experimental adsorption of olefins in aluminosilicates with different chemical compositions.

We performed an extensive study of propane/propylene separation in pure silica zeolites and aluminosilicates including LTA5A, CaA, NaY, NaX, and CaX structures. We analyzed the influence of concentration and type of cations in the separation capability of the structures. We also conducted structure minimizations using both, density functional theory (DFT) and classical optimization methods obtaining accurate models for the zeolite frameworks. We analyzed the importance of the structural optimization and the location of the cations in crystallographic positions for a correct description of the adsorption processes.

Methodology

Experimental Section

Experimental gas adsorption isotherms were performed in a volumetric analyser (3Flex, Micromeritics) provided with a turbomolecular vacuum pump and three pressure transducers (0.13, 1.33 and 133 kPa, uncertainty within 0.15% of each reading). The volumetric analyser was coupled to a thermostatic circulating bath provided with an internal sensor that allows a fine temperature control between 253–373 K with a stability of ± 0.1 K. Isotherms were recorded in the pressure range between 10-2 and 120 kPa using ca. 250 mg of sample. Before the analysis, the samples were outgassed under dynamic vacuum using a turbomolecular pump (5K/min up to 363 K for 1 hour, and then up to 623 K for 7 hours). All gases were supplied by Air Products at an ultrahigh purity (i.e., 99.995%).

For adsorption measurements of *n*-hexane and 1-hexene we used commercial zeolites 5A (CaNa-LTA, Arkema, Poland) and NaY (Si/Al ratio of 2.61, Institute of Industrial Chemistry, Poland). Structures were confirmed by analysis of X-ray diffraction patterns (XRD)recorded by a Rigaku MiniFlex powder diffractometer with Cu Kα radiation at 10 mA and 10 kV, 2θ step scans of 0.02°, and a counting time of 1 s per step. Adsorption measurements of *n*-hexane and 1-hexene were performed with the use of quasi-equilibrated temperature programmed desorption and adsorption (QE-TPDA).[24-25] QE-TPDA uses a home-made setup similar to the one exploited in temperature programmed desorption (TPD). During the measurement the adsorbate admixed to helium is flowing through the sample, while its concentration is monitored with the TCD detector. Desorption and adsorption is induced by changing of the temperature of the sample.

The studied materials were pressed into pellets, crushed and sieved to obtain fraction of 400–500 μm. Prior to each QE-TPDA measurements the sample of 10–12 mg was activated in pure helium (Air Products, purity 5.0) with flow set to 6.75 cm^3 min^{-1} by heating up to 500 °C (10 °C/min ramp). Afterwards, the sample was cooled to room temperature and the flow was switched to helium containing small admixture (0.6–0.7 mol%) of *n*-hexane (analytical pure, Acros Organics) or 1-hexene (99% Acros Organics) resulting in isothermal room temperature (RT) adsorption. When RT adsorption was finished, the actual QE-TPDA experiment was performed by cyclic heating and cooling the sample in a He/hydrocarbon flow with different rates of changing the temperature, from 2 to 10 °C/min. The sample was kept in RT for at least 2 hours between the following desorption-adsorption cycles.

The dependence of temperature on specific sorption rate (ssr) - the value proportional to the amount of desorbing/adsorption hydrocarbon - is referred as QE-TPDA profile. In order to obtain adsorption isobars, the profiles measured with the rate of changing temperature of 4 °C/min (1-hexene) or °5 C/min (*n*-hexane) were integrated and recalculated with adequate calibration constants. A detailed description of the QE-TPDA apparatus and data reduction formalism can be found in earlier works.[24-26]

Computational Details

Adsorption isotherms and isobars were calculated using grand-canonical Monte Carlo simulations (GCMC). Chemical potential and pressure are related to fugacity through the Peng-Robinson equation of state [27] and the fugacity coefficient. Simulations were performed using RASPA code.[28-29] Equimolar mixtures of propane/propylene in all pure silica zeolites were predicted using GAIAST,[30] a genetic algorithm based on ideal adsorption solution theory (IAST). In the case of competitive adsorption in aluminosilicates, we used GCMC simulations to compute the adsorption of equimolar mixtures.

During the GCMC simulations we considered the zeolites as rigid frameworks with silicon, oxygen, and aluminium atoms placed at the crystallographic positions. Extra-framework sodium and calcium cations

were allowed to move during the simulation. The point charges used for the framework atoms and extra-framework cations are collected in Table S1. Note that we used different point charges for oxygen atoms bridging one Si and one Al atom (O_{Al}), and oxygen atoms bridging two Si atoms (O_{Si}).[18] However, the set of point charges are the same for all the zeolites independently of the number Si/Al ratio (Table S1). The pure silica structures for the screening are taken from the International Zeolite Association (IZA) database.[31] The structure of LTA5A were reported by J.J. Pluth and J.V. Smith.[32] The structure of NaY and NaX were created as follows, starting with the pure silica structure. 1) Using random substitution, silicon atoms were replaced by aluminium atoms obeying Löwenstein's rule. A set of 50 structures with the same composition but different configurations was generated; 2) From the 50 structures we choose that with the most favorable (less energetic) configuration; 3) the extra-framework cations were placed in the most probable crystallographic positions reported in literature.[33-37] Schematic representation of FAU-type, and LTA-type zeolites and the description of the cations sites can be found in Figure S1 of the ESI. We created the CaX and the CaA structures by placing the calcium cations in the structure of NaX and LTA5A, respectively. Classical structural minimizations of the aluminosilicates with the cations placed in the crystallographic positions were performed using Baker's method [38] and the well-known core-shell potential of Sanders et al.[39-40] We carried out simulations in NPT ensemble, that allows the variation of box lengths (i.e. the volume of the cell) but keeping fixed the angles ($\alpha=\beta=\gamma=90^{o}$) to maintain the triclinic crystal system.

Adsorbates are described using united atom models, where each CH_n group is considered as a single interaction center. Propane and longer linear paraffins are modeled as non-polar molecules and their interaction parameters were taken from Dubbeldam et al.[18, 21, 41] For propylene we compare the accuracy of a non-polar model reported by Liu et. al.[42] and a point charge model with partial charges located in CH_n_sp^2 groups and one extra point charge between the two carbon atoms linked by the double bond. The latter model was developed and validated by Gutierrez-Sevillano et. al.[8] and can be extended to longer α-olefins in a simple way. Figure S2 shows the good agreement between our experimental and simulation data with these taken from the literature.[43-45] The Lennard-Jones (LJ) interaction parameters for sp^3 carbon atoms, extra-framework cations, and the zeolite atoms are taken from reference.[18] The interaction parameters for sp^2 carbon atoms of non-polar and point charge propylene with silica and oxygen zeolite atoms are also taken from the literature.[8, 42] The new set of parameters for sp^2 carbon atoms and extra-framework cations were developed to reproduce the experimental isotherms. To this aim, we fit the potential parameters of the cross interactions between propylene and sodium cations in NaY zeolite at room temperature. Once validated, we used this new set of parameters to fit the interaction of propylene with calcium cations in LTA5A. We validated the model by comparing with experimental adsorption isotherms measured in this work and comparing with independent experiments found in literature.[13, 46-48] We checked the transferability of the set of parameters by computing adsorption isotherms in other zeolites and for α-olefins with longer chains. The LJ parameters developed in this work are collected in Table S1 in the Supporting Information. We computed the binding geometries using the classical force field by a simulated annealing process based on molecular dynamics (MD) simulations in the NVT ensemble. During this process, we started with zeolites loaded at 273 K and 1 bar. Then, the temperature was reduced in intervals of 10 degrees until 3 K and then until 1 K. With this procedure we minimized the effect of temperature on the vibration of the molecules making more accurate the comparison with the DFT calculations. We run each MD simulation for 10^6 steps and using a time step of 0.5 fs. More details about the MD methodology can be found in ref.[7]

In addition to classical simulations, we performed density functional theory (DFT) calculations to optimize the structure of LTA5A and NaY zeolites. The geometry of these zeolites were fully optimized using the Vienna ab initio simulation package (VASP) code,[49-52] employing the generalized gradient approximation (GGA) with the Perdew-Burke-Ernzerhof exchange-correlation functional [53] and projector-augmented wave (PAW) potentials.[54-55] Valence electrons are described using a plane-wave basis set with a cutoff of 500 eV and the gamma point is used for integrations in the reciprocal space.[56] The ionic relaxation has been performed until the Hellmann-Feynman forces were lower than 0.02 eV/Å. We compared the resulting structures from the classical and DFT optimization methods. In addition to the

geometry optimization, we also computed the binding energy and binding geometry of a single molecule of propane and propylene in the two mentioned zeolites. Van der Waals interactions were taken into account through the DFT-D2 method of Grimme [57] to gain insights into the particular interaction between the alkene molecules and the monovalent and divalent cations of the zeolites. The position of the molecule was optimized keeping the zeolite atoms and the cations in the previously optimized positions. As these results can be influenced decisively by the starting geometry, we used several starting geometries for each molecule to ensure stability. We used the strategy of performing preliminary short *ab-initio* MD simulations at low temperature to identify the most stable configuration prior to start the optimizations.

Results and Discussion

Propane and propylene adsorption in pure silica zeolites

To identify the optimal topology for propane/propylene separation, we used the models and force field from the literature [8, 21] to calculate the adsorption isotherms of propane and propylene in most zeolites of the IZA database in the pure silica form (more than 200 topologies). Adsorption selectivity was used as a measure of the separation factor of the mixture. Adsorption selectivity is defined as $S = (x_A/y_A)/(x_B/y_B)$were x_i is the molar fraction in the adsorbed phase for the component *i* and y_i is the molar fraction in the bulk phase. Figure 1 shows the adsorption selectivity as a function of the pore volume at 100 kPa and 298 K, for the studied zeolites. For clarity purposes, we have classified the zeolite structures in those exhibiting preferential adsorption for propane (Figure 1a) or for propylene (Figure 1b).

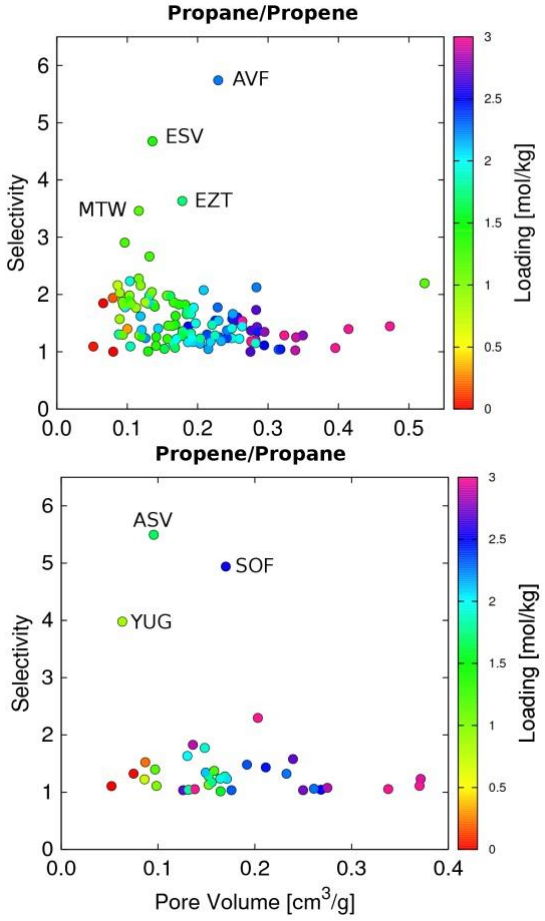

Figure 1. Adsorption selectivity as a function of pore volume for (top) propane over propylene and (bottom) propylene over propane at 298 K and 100 kPa for the studied zeolites. Color scale (right Y axis) represents the total amount adsorbed in the gas phase.

The selectivity obtained for most zeolites in these conditions is quite low (below 2) and only for a few of them is higher than 3. AVF, EZT, ESV, and MTW exhibit high adsorption selectivity for propane over propene, whereas ASV, SOF, and YUG show higher selectivity for propylene over propane. Among them, the only zeolite that is available in pure silica form is MTW, and the uptake is about 1 mol/kg in the studied conditions. Therefore, olefin/paraffin separation based on pure silica zeolites seems inefficient and unrealistic. To improve this separation it is necessary to take advance of other mechanisms which makes the difference between olefins and paraffins.

Effect of cations in the adsorption

It is well known that π-complexation (also known as π-bonding) enhances olefin/paraffin separation.[58-61] π-complexation is a subgroup of chemical complexation where a covalent bond is formed between the electron donor (olefin) and the acceptor (complexing agent). [62] This phenomenon occurs in Metal-Organic Frameworks with open metal sites and it is also reported in zeolites with complexing agent which is usually a member of the d-block transition metals in the periodic table. The π-complexation formed stronger bonds than van der Waals forces, so it is possible to achieve higher adsorption selectivity and higher adsorption capacities.[63-66] Similarly, π-complexation can also occur in aluminosilicates due to the interaction of olefins with the extraframeworks cations.[58, 60-61] The effect of the π-complexation results in differences in the adsorption properties of olefins and paraffins. To gain insights into these differences we measured the adsorption properties of olefins and paraffins in aluminosilicates containing sodium (NaY) and sodium and calcium cations (LTA5A).

First of all, we measured the QE-TPDA profiles of n-hexane and 1-hexene in NaY (Na-FAU, Si/Al=2.61) and LTA5A (CaNa-LTA, Si/Al=1) zeolites (Figure 2). QE-TPDA profiles should show similar behaviour for two adsorbate-adsorbent pairs when the adsorbed molecules have similar affinity to the structure. As seen, dissimilar profiles are obtained for olefin and paraffin, which is an indication of the mentioned π-complexation between the olefin and the cations.

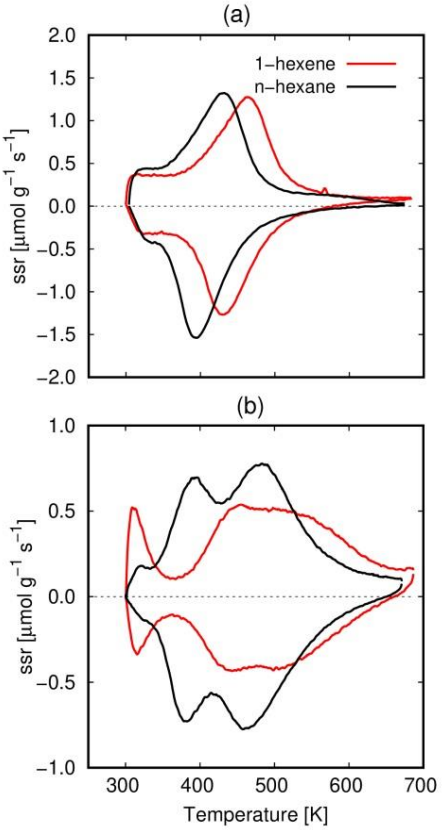

Figure 2. QE-TPDA profiles of *n*-hexane and 1-hexene in (a) NaY and (b) LTA5A. The partial pressure of *n*-hexane in NaY and LTA5A was *ca* 790 Pa and 680 Pa, respectively. For 1-hexene in NaY and LTA5A it was *ca* 560 Pa and 570 Pa, respectively.

The profiles consist of desorption maxima and adsorption minima, which corresponds to the instantaneous amount of the component desorbing/adsorption in the material at given conditions. Desorption maxima are slightly shifted to higher temperatures when compared to adsorption minima, which is apparatus artifact. For adsorption of *n*-hexane and 1-hexene in NaY we observe sharp peaks, which for 1-hexene are shifted by ca. 35 K to higher temperatures. The higher desorption/adsorption

temperatures of 1-hexene most likely result from stronger interactions of the olefin molecules with sodium cations. The low temperature range of the profiles (300-350 K) corresponds to dense adsorption states related to guest-guest interactions. While the QE-TPDA profiles of *n*-hexane and 1-hexene in NaY are quite similar, they significantly differ for LTA5A. For *n*-hexane in LTA5A we observe two clear desorption/adsorption peaks in the range of 350-550 K. As for NaY, the profiles of 1-hexene in LTA5A are shifted to the higher temperature, but they also differ in shape as we observe a wide signal extending from 400 to 650 K. The low-temperature peak at 315 K is separated from the rest of the profile, which may suggest noticeable difference between guest-guest and guest-host interactions of 1-hexene in LTA5A zeolite than in NaY. Summarizing the QE-TPDA results, 1-hexene is adsorbed at markedly higher temperature than *n*-hexene in both NaY and LTA5A zeolites. Moreover, the differences in the profiles are more relevant for LTA5A zeolite indicating that the calcium cations influence more than the sodium cations in the adsorption process.

Fitting Interaction between cations and CH_n_sp2 groups. To gain insights into the differences in the adsorption of olefins and paraffins in aluminosilicates, we combined experimental and molecular simulation techniques. Molecular simulations offer useful information of the adsorption process from a microscopic point of view. As described in the methodology, we used previously validated force fields to study the adsorption of paraffins in aluminosilicates. However, there are not a transferable potential for the interaction of olefins with the extraframework sodium and calcium cations. In addition to the isobaric adsorption of 1-hexene, we measured the adsorption isotherms of propylene in the same adsorbents. We used these experimental values as reference to develop a set of effective potential parameters to study the adsorption process.

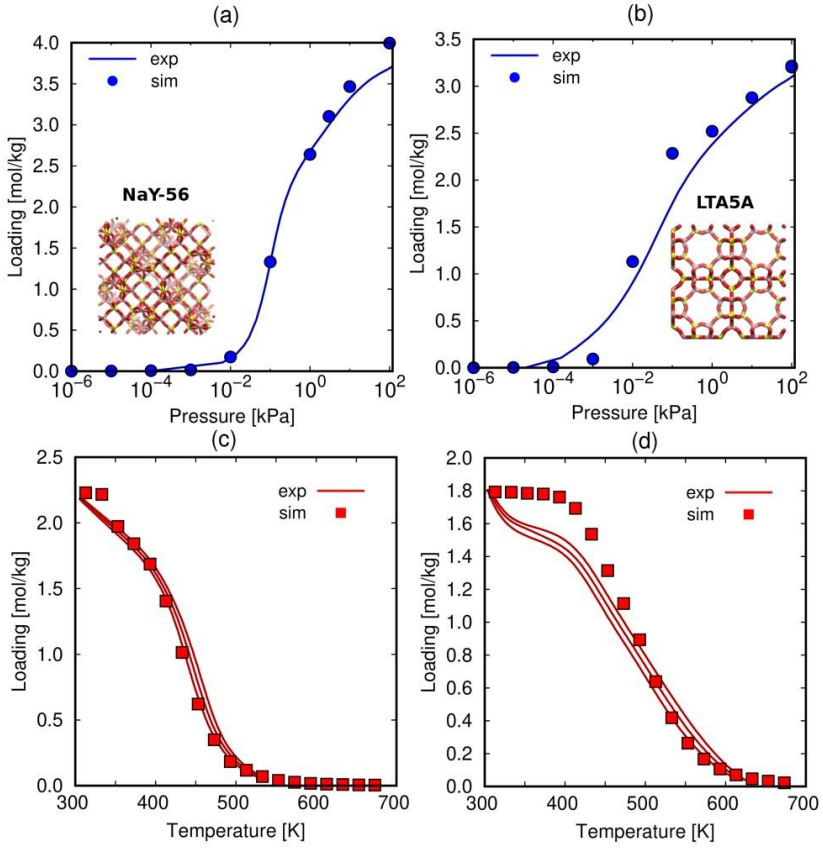

Figure 3. Adsorption isotherms of propylene in (a) NaY-56 and (b) LTA5A at 298 K. Adsorption isobars of 1-hexene in (c) NaY-56 at 560 Pa and (d) LTA5A at 550 Pa. Experimental results are represented with lines and calculated results with symbols. For isobars three curves are plotted, the curve shifted to the highest and lowest temperatures stand for desorption and adsorption, respectively. Averaging the adsorption and desorption curves we obtain the adsorption isobar reflected as the intermediate curve.

The particular interaction between extra-framework cations and olefins through the double bond makes challenging to reproduce the adsorption experiments using molecular simulations. We developed a set of Lennard-Jones parameters for the interaction between $CH_n\_sp^2$ groups and Na^+ extra-framework cations by fitting to the experimental adsorption isotherm of propylene in CBV100 (NaY with Si/Al=2.55) at 298 K (Figure 3a). Once these values were fixed, we fit the Lennard-Jones parameters for the interaction between $CH_x\_sp^2$ groups and Ca^{2+} using the experimental adsorption isotherm of propylene in LTA5A zeolite (Figure 3b). To check if the model can be applied to longer molecules, we compared the computed and the measured adsorption isobars of 1-hexene in NaY (Na-FAU, Si/Al=2.61) and LTA5A (CaNa-LTA, Si/Al=1) zeolites at 560 Pa and 570 Pa, respectively. As shown in Figure 3c,d, we found a good agreement between experiments and simulations. Comparison with other experimental values reported for propylene and 1-butene in NaY, NaX, and LTA5A at several temperatures [13, 46, 48] can be found in Figure S3 and S4 of the ESI. The good agreement verifies that our set of Lennard-Jones parameters reproduce experimental adsorption isotherms and isobars of olefins (propylene and long chain hydrocarbons) and it is transferable to zeolites of different topology and to many operational values of temperature. Note that with the same force field we reproduced the experimental adsorption isobars and isotherms from this work and from the literature, which were measured with different samples, equipment and methodology. This gives consistency to the experimental measurements performed in this work.

Energies and Binding geometries

Differences in the adsorption of olefins and paraffins in aluminosilicates are also reflected in the binding energies and in the structural organization of the adsorbates in the cavities of the zeolites. Binding or adsorption energies were obtained with DFT calculations of a single molecule of propane and propylene in NaY and LTA5A. The binding energies of propane and propene in NaY are -0.469 eV and -0.590 eV, respectively. The adsorption energy of propane in LTA5A is -0.694 eV, which is an average of the interaction with Ca^{2+} and Na^+ cations. However, the structure containing propylene shows two favorable configurations: one when the molecule is near to the sodium cations and other near to calcium cations. In this case we found strong interactions between the molecule and the calcium cations which were missing during propane adsorption. When the molecule of propylene is near the Na^+ cation, the adsorption energy is very similar to the propane adsorption energy (-0.667 eV) but when propylene is adsorbed near the Ca^{2+} cation the adsorption energy is -0.885 eV. This indicates that at low coverage propylene adsorbs preferentially binding to the calcium cations. In the two zeolites, propylene shows higher adsorption energy than propane. The differences in the adsorption energy between propylene and propane are 0.121 eV for NaY and 0.191 eV for LTA5A. The larger difference in energy showed by LTA5A compared to NaY is due to the presence of calcium cations, which is consistent with the huge differences observed in the QE-TPDA profiles (Figure 2).

The binding geometry of these adsorbates in the zeolite pores is also key factor to describe correctly the adsorption properties. From the same DFT calculations we also obtained the binding geometries for propane and propylene. The most stable configuration of the molecule of propane in LTA5A is between one calcium and one sodium atom, independently of the starting position of the molecule. In the optimized LTA5A the distances between one of the terminal carbon atom of propane and the Na^+ cation is 2.97 Å and the distance between the other terminal carbon atom of the molecule and the Ca^{2+} cation is 2.91 Å. The terminal carbon of propane atom is pointing to the cations forming an angle of about 170º. We found similar orientation of propane in NaY, with the same angle but the distance between the terminal carbon atom and the Na^+ cation is 2.68 Å. In the case of propylene, we found a different behaviour of the structural organization of the adsorbate with respect to the cations. We quantify the binding geometry of propylene by defining the parameters d_1, d_2, and α according to the schematic representation of Figure 4a. d_1 is the distance between the terminal carbon atom ($CH_2\_sp^2$) with the cation, d_2 the distance of the central carbon atom with the cation, and α is the angle between the double bond and d_1. The propylene-Na^+ distances are similar for both structures; d_2 is slightly larger in NaY than in LTA5A, which also implies larger α. The double bond is located approximately "parallel" to the cation (α ~ 90º) in NaY while in LTA5A α is about 80º. To check the accuracy of the classical force field to

reproduce the binding geometry, we computed the radial distribution functions RDFs between the atoms which define d_1 and d_2.

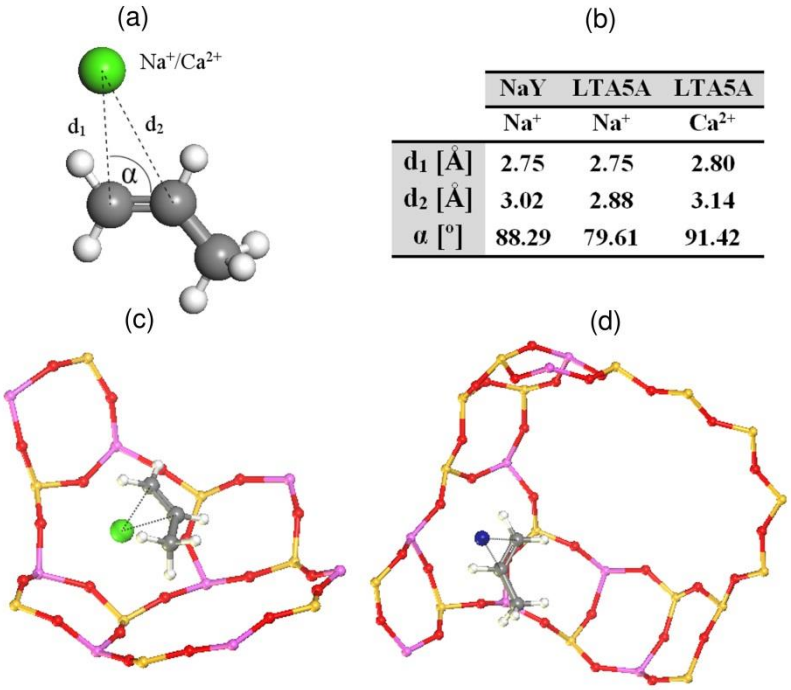

	NaY	LTA5A	LTA5A
	Na^+	Na^+	Ca^{2+}
d_1 [Å]	2.75	2.75	2.80
d_2 [Å]	3.02	2.88	3.14
α [°]	88.29	79.61	91.42

Figure 4. (a) Schematic representation of the parameters used to describe the binding geometry, (b) binding geometry of propylene with sodium and calcium cations obtained with DFT calculations, and schematic representation of the most favorable configuration of propylene in (c) LTA5A and (d) NaY.

Figure 5 compares these parameters obtained with DFT calculations with the RDFs from a classical MD simulation after a simulated annealing procedure. We obtained similar orientations of the molecule in the two structures with the mentioned techniques. The first peak of the RDF matches with the given distances by the DFT calculations. The largest displacement (0.3 Å) is found for d_1 for calcium cation in LTA5A.

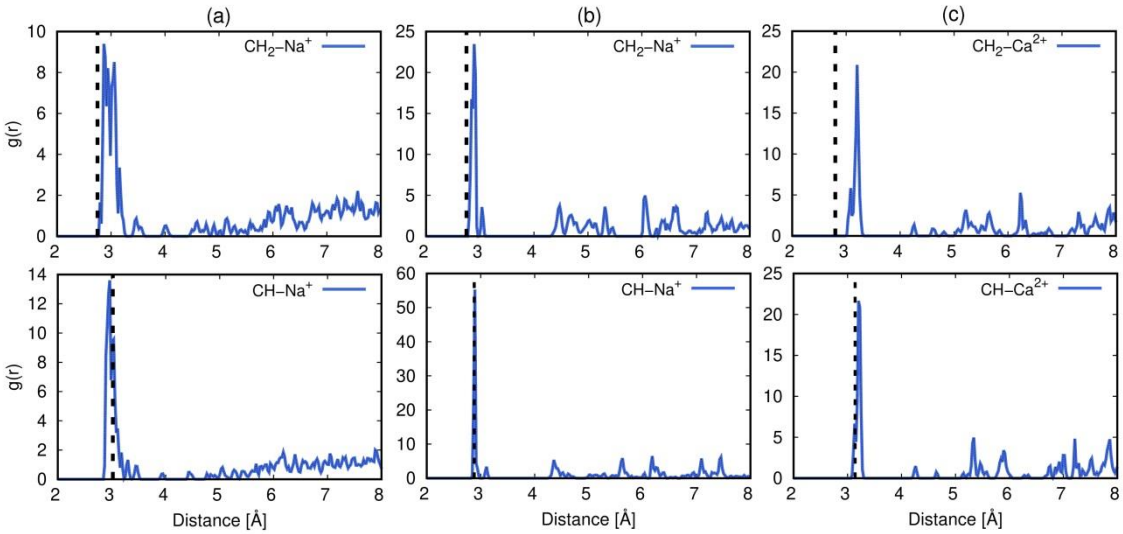

Figure 5. (a) Comparison of the binding geometry parameters d_1 (top) and d_2 (bottom) obtained with DFT (dashed vertical lines) and classical simulation (blue solid lines) of propylene with cations in (a) NaY and (b), (c) LTA5A. The parameters are used according to the schematic representation of Figure 4a.

We found that propane and propylene molecules orientate differently with respect to the cations (complexing agent), which is in agreement with the reported binding geometry for olefins in MOFs with open metal sites. In these systems, the double bond is located parallel to the metal ($\alpha \approx 90^{o}$) for olefins but the angle is larger for paraffins.[61, 65, 67] These results reinforce the validity of our set of Lennard-Jones parameters for olefins in aluminosilicates.

We analyzed the microscopic organization of the olefins as increasing the amount adsorbed. In NaY, propylene molecules are located closed to the sodium atoms. However, in LTA5A the location of propylene near calcium or sodium cations depends on the quantity adsorbed. Figure 6 shows the most probable distance between the central carbon atom and the cation (average of d_2 over all the adsorbed molecules) as a function of the loading in LTA5A at 298K. At low loading the adsorbed molecule is placed near the Ca^{2+} (circles) cations at a distance of 3.2 Å. This value remains constant with loading. On the other hand, the most probable distance between the central carbon atom and the Na^{+} cations (triangles) at low loading is about 5.5 Å which is also the distance between nearest Na^{+} and Ca^{2+} cations. The distance remains constant up to 32 molecules per unit cell. At higher values of loading this distance decreases up to 2.9 Å. According to the first peak of the RDFs of Figure 6 (bottom), propylene molecules locate close to calcium cations independently of the loading. However, there is no significant presence of propylene near sodium cations at low or intermediate coverage (low intensity first peaks, below the unity, of the RDF). When the loading of propylene exceeds the value of 32 molecules per unit cell, the first peak of RDF corresponding to CH-Na^{+} shows a drastic increase. Note that the number of calcium cations per unit cell in LTA5A is 32. This means that once all the calcium cations are surrounded by propylene molecules, they begin to adsorb near to the sodium cations.

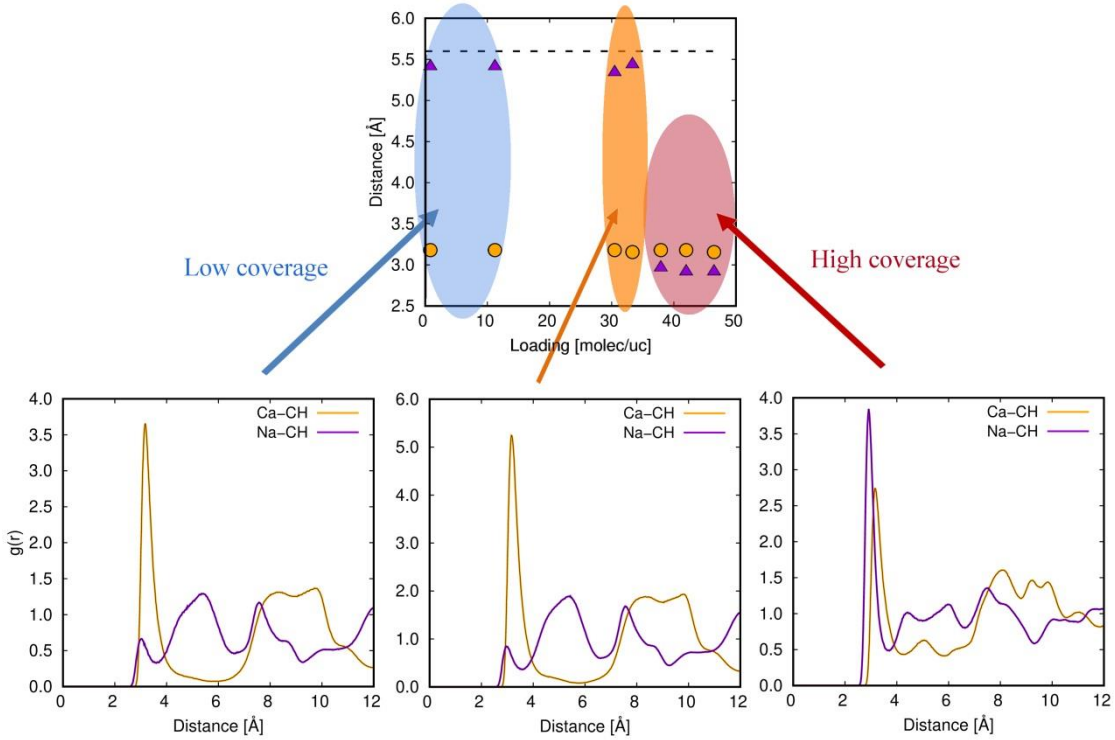

Figure 6. (Top) The most probable distance between CH pseudo-atom and Na^{+} (purple triangles) and Ca^{2+} cations (orange circles) as a function of loading in LTA5A. Dashed line indicates the shorter distance between Na^{+} and Ca^{2+} cations. (Bottom) RDF of CH pseudo-atom with cations at low coverage (left), medium coverage (center) and close to saturation (right).

Effect of the structural optimization

Following the procedure explained in the methodology, we optimized the structures of the NaY and LTA5A zeolites using DFT and classical simulations to study the effect of the geometry. Then we computed adsorption isotherms and isobars of propane and propylene. Figure 7 shows a schematic representation of the 4-, 6-, 8-, and 12-member ring (MR) present in these aluminosilicates and the distances are summarized in Table 1.

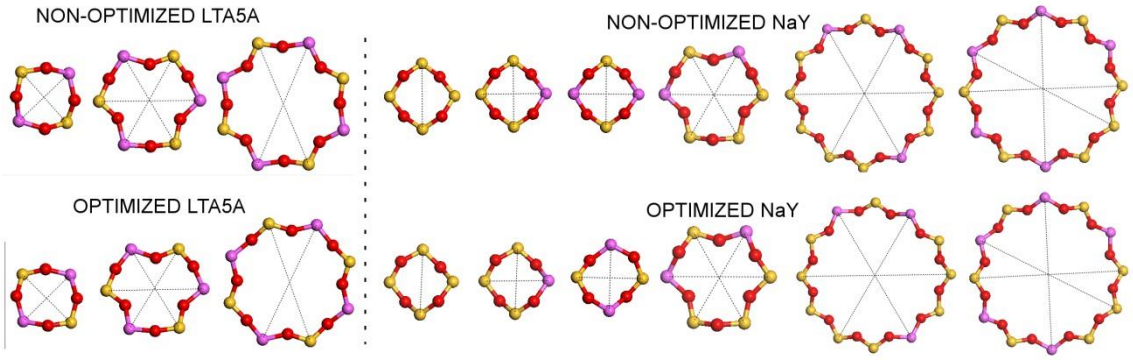

Figure 7. Schematic representation of 4-, 6-, 8-, and 12-member ring of non-optimized and classically optimized LTA5A and NaY structures. Dashed lines indicate the selected distances for the data listed in Table 1.

Table 1. Comparison of the unit cell and the distances between the atoms of the member ring for non-optimized and classically optimized structures.

		Distance [Å] Non-optimized structure	**Distance [Å]** Optimized structure
LTA5A			
Unit cell	a=b=c	24.7484	24.7529
4MR	Si-Si	4.56	4.56
	Al-Al	4.4	4.41
6MR	Al-Si	6.46	6.45
	Al-Si	6.46	6.45
	Al-Si	6.46	6.45
8MR	Si-Si	8.34	8.39
	Al-Al	8.42	8.5
NaY			
Unit cell	a=b=c	24.555	24.6668
4MR	Si-Si(Al=0)	4.45	4.37
	Si-Si(Al=1)	4.45	4.43
	Si-Al(Al=1)	4.39	4.37
	Si-Si(Al=2)	4.45	4.46
	Al-Al(Al=2)	4.39	4.36
6MR	Si-Si	6.29	6.27
	Al-Si	6.29	6.25
	Si-Al	6.29	6.28
12MR	Si-Si(Al=3)	11.62	11.77
	Al-Al(Al=3)	11.62	11.54
	Si-Al(Al=3)	11.62	11.55
	Si-Si(Al=5)	11.62	11.53
	Al-Al(Al=5)	11.62	11.68
	Si-Al(Al=5)	11.62	11.58

One can observe that there are tiny differences between the non-optimized and optimized building units of the zeolites. To corroborate it, we compared the experimental and the calculated XRD diffractograms (see Figure S5 of the ESI). Our results show that there are non-significant displacement of the peaks in the pattern of the non-optimized and the optimized structures. Then we conclude that the discrepancies in distances between adjacent planes are negligible between the different models for LTA5A and NaY. Nevertheless we found large variations in the adsorption of propylene and 1-hexene. Figure 8 illustrates the adsorption isotherms of propane, and propylene in LTA5A and NaY zeolites in the i) non-optimized and ii) optimized structures using DFT calculations, and iii) in optimized structures with classical simulations. The adsorption of propane in NaY and LTA5A is similar in all the structures, in agreement with the experimental values. The main differences in the loading are found in the region of the inflection point of the isotherm, due to the small variation of the intracrystalline distances of the zeolites. On the other hand, the adsorption isotherms of propylene calculated in the non-optimized NaY and LTA5A zeolites do not match experimental data, while computed isotherms in the optimized structures are in better agreement with experiments. We analyzed the adsorption of *n*-hexane and 1-hexene in the optimized and non-optimized frameworks (Figure S6 in the ESI) and obtain similar conclusions. This means that the optimization of the structure is not needed for the adsorption of paraffins, but increase significantly the accuracy of the predictions for the adsorption of olefins in aluminosilicates. Small deviations of a given atom of the structure can produce changes in the electrostatic field inside the cavities affecting the olefin adsorption; however, this is irrelevant for the adsorption of paraffins.

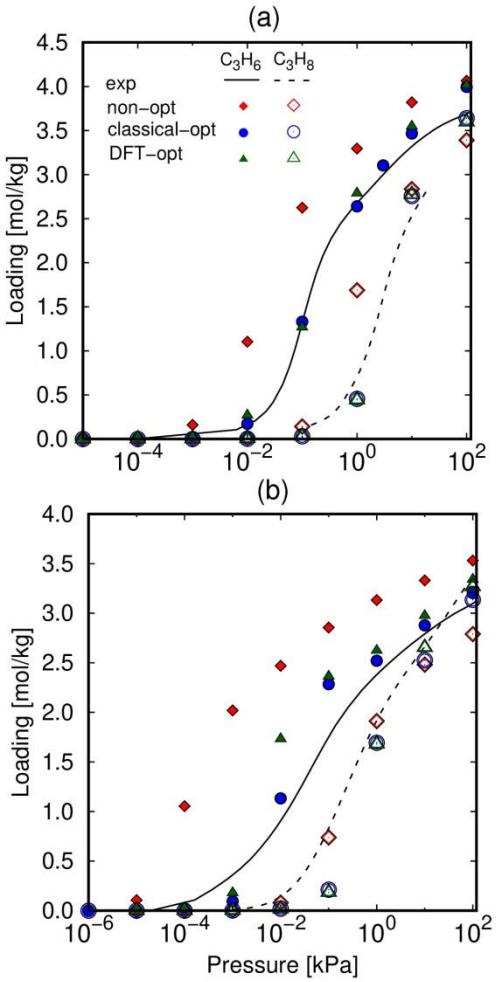

Figure 8. Comparison between adsorption isotherms (298 K) of propane (open symbols) and propylene (closed symbols) in (a) NaY and (b) LTA5A using non-optimized structures (red diamonds), DFT optimized structures (green triangles) and classically optimized structures (blue circles). Experimental data are represented by solid lines (this work) and dashed lines (literature).[68-69]

Effect of cations in the separation

We have shown how calcium cations of LTA5A interact more strongly with olefins than sodium cations. Then we also include in this study, the aluminosilicates based only in calcium cations, such as CaA and CaX with LTA and FAU topologies, respectively. The influence of the nature of the cation in the adsorption can be observed in the average occupation profiles (AvOPs). Figure 9 shows the AvOPs of propylene in zeolites with FAU topology (FAU-Si, NaY, NaX, and CaX) at 100 kPa and 298 K. At these conditions, the four structures have the same loading, but the preferential adsorption sites differ. The pure silica zeolite shows preferential adsorption in the center of the cages, and almost a homogenous distribution in the rest of the cavity. In the NaY and NaX structures, the Na^+ cations become new adsorption sites. These preferential sites allow for more heterogeneous distribution of the molecules during adsorption. The centers of the cages are practically non-occupied in presence of Ca^{2+} cations while the distribution of the adsorbed molecules of propylene is close to the cations. NaY and CaX have similar number of cations in the simulation box; 56 and 48, respectively. Thus the main difference in their occupation profiles is due to the type of cation (Na^+ or Ca^{2+}) and the location of the cations in the structure. The average occupation profiles obtained for the different compositions in LTA topology are provided in Figure S7 in the ESI.

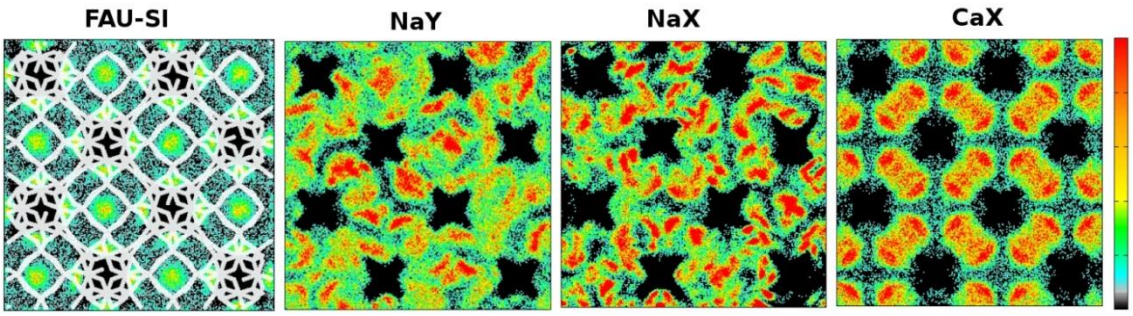

Figure 9. Average occupation profiles of propene in FAU topology at 100 kPa and 298 K.

To quantify the effect exerted by the calcium cation in the separation of the paraffin/olefin mixture, we performed equimolar adsorption isotherms of propane/propylene mixture in zeolites with FAU topology (FAU-Si, HS-FAU, NaY, NaX, and CaX) and with LTA topology (ITQ-29, LTA5A, and CaA). Figure 10 shows that zeolites CaX and CaA are excellent candidates to separate propane from propylene. As seen, the calcium forms of these zeolites adsorb more than 3 mol/kg of propylene, while propane is almost excluded from the mixture. The other structures with cations are also good candidates for separation as can be observed in Figure S8 (ESI). As we have demonstrated before, this exceptional separation is a consequence of the strong interaction of the olefins with the cations. The π-complexation between propylene and the extraframework cations makes the difference for the separation of propylene/propane in zeolites. To analyze the effect of the length of the alkyl chain in the olefin/paraffin separation, we extended our study to longer hydrocarbons. Figure 11 shows the olefin/paraffin adsorption selectivity as a function of the chain length in FAU and LTA type zeolites. This was obtained from the equimolar adsorption isotherms of olefin/paraffin pairs from C3 to C9 carbon atoms at 100 kPa and 298 K. As for propylene/propane, ITQ-29 (pure silica with LTA topology), FAU-Si (pure silica) and HS-FAU (high silica with a Si/Al ratio ≈ 100) cannot separate the olefin/paraffin mixtures. In NaY (circles) the adsorption selectivity in favor of the olefin is about 10 for all chain lengths, and the highest separation is obtained for C6 (1-hexene/*n*-hexane) with a selectivity value of 25. The pair olefin/paraffin with the highest values of adsorption selectivity depends of the density of the cations. The best separation performance in most FAU-type zeolites is found for the C6 mixture. In NaX zeolite separation is better for C5 (selectivity ≈ 90). NaX (diamonds) and LTA5A (squares) show similar behavior with very similar selectivity for all the pairs. As mentioned before, CaX (triangles) shows similar selectivity for propane/propylene separation than NaY, but the increase of the selectivity is not linear with increasing the chain length. We found a maximum for the C6 mixture and also good separation performance for the

mixtures C7, C8 and C9. CaA is the zeolite with the best olefin/paraffin separation performance for all pairs. The separation values are particularly high for the C3, C4, C5, and C6 mixtures. On the other hand, FAU and LTA-type zeolites have similar adsorption capacity, represented by the color scale in Figure 11. LTA5A and CaA shows olefins storage of about 150-170 mg/g while the other aluminosilicates with FAU topology show higher capacity (about 185 mg/g). In general, an increase in the length of the hydrocarbon mixture up to 9 carbon atoms does not lower the separation performance of aluminosilicates. This makes these materials excellent candidates for the targeted separation.

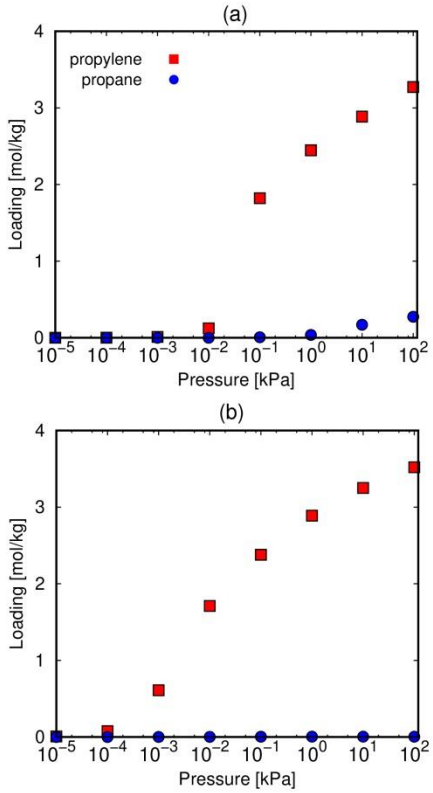

Figure 10. Equimolar adsorption isotherms of propane/propylene in (a) CaX and (b) CaA zeolites at 298 K.

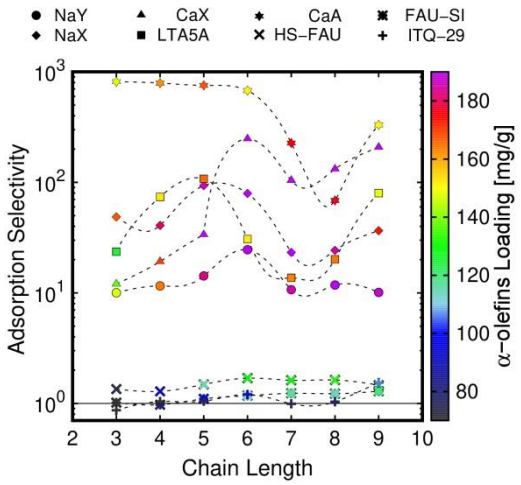

Figure 11. Adsorption selectivity of binary mixture (from C3 to C9) as a function of chain length in FAU and LTA frameworks at 100 kPa and 298 K. Color scale represents the amount of olefins adsorbed.

CONCLUSIONS

We studied the olefin/paraffin separation of hydrocarbons with three to nine carbon atoms, with a combination of experimental and molecular simulation techniques. Separation of equimolar binary mixtures was predicted from the screening of the adsorption isotherms of pure components in more than 200 structures. This allowed the analysis of the effect of the zeolite topology in the propane/propylene separation in pure silica zeolites. Adsorption selectivity confirmed that pure silica zeolites cannot be used to separate these mixtures. Only in a few structures the values of adsorption selectivity were above 3 at room conditions, but in general, the adsorption capacity of these structures is extremely low. To achieve olefin/paraffin separation using zeolites, aluminosilicates with extra-framework cations that interact strongly with the olefins are needed.

Experimental adsorption measurements of propylene in commercial NaY and LTA5A zeolites at different temperatures allowed us to develop a set of Lennard-Jones parameters for the specific interactions between the extra-framework cations and the $CH_n\_sp^2$ pseudo-atom groups of olefin models. These parameters provided good agreement between the experimental and computational adsorption isotherms of propylene for a wide range of temperatures and a variety of cationic zeolites. Comparison with adsorption isobars of 1-hexene in NaY and LTA5A measured in this work confirmed the transferability of these force field parameters to longer hydrocarbons. We also found that for reproducing the adsorption of olefins in aluminosilicates the location of the cations and the optimization of the structures are key factors.

In aluminosilicates, π-bonding is formed between double bond of the propylene molecule and one accessible Na^+ or Ca^{2+} cation. DFT calculations showed that the binding energies in NaY and LTA5A for propylene are much higher than the obtained for propane. The preferential adsorption sites are close to the cations and in particular, close to the Ca^{2+} cations in LTA5A. The binding geometries reflect the differences between propane and propylene too. The double bond is oriented in parallel to the cation forming an angle of about 90º while for propane the terminal carbon atom is pointing to the cation and α is about 170º. We found agreement between the binding geometries obtained with DFT and with classical calculations. In conclusion, zeolites with cations are excellent candidates for olefin/paraffin separation due to the strong interaction of the olefin with the cation though the π-bonding. The binding energies indicate that this interaction is stronger with divalent cations, such as calcium. Therefore, exchanging Na^+ cations for Ca^{2+} cation in zeolites might enhance the olefin/paraffin separation with an exclusion of the paraffin from the mixture.

Akcnowledgements

This work was supported by the Spanish Ministerio de Economía y Competitividad (CTQ2016-80206-P). We thank C3UPO for the HPC support. A. Luna-Triguero and J. M. Vicent-Luna thank to Santander Universidades for their *Beca Iberoamérica Santander Investigación*. Andrzej Sławek obtained financial resources as part of financing the doctoral scholarship from the National Science Center, Poland Grant No. 2018/28/T/ST5/00274.

References

1. Park, Y.-K.; Lee, C. W.; Kang, N. Y.; Choi, W. C.; Choi, S.; Oh, S. H.; Park, D. S., Catalytic Cracking of Lower-Valued Hydrocarbons for Producing Light Olefins. *Catalysis surveys from Asia* **2010**, *14*, 75-84.
2. Wagner, H.; Luther, R.; Mang, T., Lubricant Base Fluids Based on Renewable Raw Materials: Their Catalytic Manufacture and Modification. *Appl. Catal., A* **2001**, *221*, 429-442.
3. Alsadoun, A. W., Dimerization of Ethylene to Butene-1 Catalyzed by Ti(or')4-Alr3. *Appl. Catal., A* **1993**, *105*, 1-40.
4. Eldridge, R. B., Olefin Paraffin Separation Technology - a Review. *Ind. Eng. Chem. Res.* **1993**, *32*, 2208-2212.
5. Gascon, J.; Blom, W.; van Miltenburg, A.; Ferreira, A.; Berger, R.; Kapteijn, F., Accelerated Synthesis of All-Silica Dd3r and Its Performance in the Separation of Propylene/Propane Mixtures. *Microporous Mesoporous Mater.* **2008**, *115*, 585-593.

6. Olson, D. H.; Yang, X.; Camblor, M. A., Itq-12: A Zeolite Having Temperature Dependent Adsorption Selectivity and Potential for Propene Separation. *J. Phys. Chem. B* **2004**, *108*, 11044-11048.
7. Min, J. G.; Luna-Triguero, A.; Byun, Y.; Balestra, S. R.; Vicent-Luna, J. M.; Calero, S.; Hong, S. B.; Camblor, M. A., Stepped Propane Adsorption in Pure-Silica Itw Zeolite. *Langmuir* **2018**, *34*, 4774-4779.
8. Gutiérrez-Sevillano, J. J.; Dubbeldam, D.; Rey, F.; Valencia, S.; Palomino, M.; Martín-Calvo, A.; Calero, S., Analysis of the Itq-12 Zeolite Performance in Propane− Propylene Separations Using a Combination of Experiments and Molecular Simulations. *J. Phys. Chem. C* **2010**, *114*, 14907-14914.
9. Hosseinpour, S.; Fatemi, S.; Mortazavi, Y.; Gholamhoseini, M.; Ravanchi, M. T., Performance of Cax Zeolite for Separation of C2h6, C2h4, and Ch4 by Adsorption Process; Capacity, Selectivity, and Dynamic Adsorption Measurements. *Sep. Sci. Technol.* **2010**, *46*, 349-355.
10. Campo, M.; Ribeiro, A.; Ferreira, A.; Santos, J.; Lutz, C.; Loureiro, J.; Rodrigues, A., New 13x Zeolite for Propylene/Propane Separation by Vacuum Swing Adsorption. *Sep. Purif. Technol.* **2013**, *103*, 60-70.
11. Lamia, N.; Wolff, L.; Leflaive, P.; Leinekugel-Le-Cocq, D.; Sá Gomes, P.; Grande, C. A.; Rodrigues, A. E., Equilibrium and Fixed Bed Adsorption of 1-Butene, Propylene and Propane over 13x Zeolite Pellets. *Sep. Sci. Technol.* **2008**, *43*, 1124-1156.
12. Calleja, G.; Jimenez, A.; Pau, J.; Dominguez, L.; Perez, P., Multicomponent Adsorption Equilibrium of Ethylene, Propane, Propylene and Co2 on 13x Zeolite. *Gas Sep. Purif.* **1994**, *8*, 247-256.
13. Grande, C. A.; Gigola, C.; Rodrigues, A. E., Adsorption of Propane and Propylene in Pellets and Crystals of 5a Zeolite. *Ind. Eng. Chem. Res.* **2002**, *41*, 85-92.
14. Dzhigit, O.; Kiselev, A.; Mikos, K.; Muttik, G.; Rahmanova, T., Heats of Adsorption of Water Vapour on X-Zeolites Containing Li+, Na+, K+, Rb+, and Cs+ Cations. *Transactions of the Faraday Society* **1971**, *67*, 458-467.
15. Harper, R.; Stifel, G.; Anderson, R., Adsorption of Gases on 4a Synthetic Zeolite. *Can. J. Chem.* **1969**, *47*, 4661-4670.
16. Grande, C. A.; Gigola, C.; Rodrigues, A. E., Propane–Propylene Binary Adsorption on Zeolite 4a. *Adsorption* **2003**, *9*, 321-329.
17. Granato, M. A.; Vlugt, T. J.; Rodrigues, A. E., Molecular Simulation of Propane− Propylene Binary Adsorption Equilibrium in Zeolite 4a. *Ind. Eng. Chem. Res.* **2007**, *46*, 321-328.
18. Calero, S.; Dubbeldam, D.; Krishna, R.; Smit, B.; Vlugt, T. J. H.; Denayer, J. F. M.; Martens, J. A.; Maesen, T. L. M., Understanding the Role of Sodium During Adsorption: A Force Field for Alkanes in Sodium-Exchanged Faujasites. *J. Am. Chem. Soc.* **2004**, *126*, 11377-11386.
19. Maesen, T. L. M.; Beerdsen, E.; Calero, S.; Dubbeldam, D.; Smit, B., Understanding Cage Effects in the N-Alkane Conversion on Zeolites. *J. Catal.* **2006**, *237*, 278-290.
20. Luna-Triguero, A.; Gómez-Álvarez, P.; Calero, S., Adsorptive Process Design for the Separation of Hexane Isomers Using Zeolites. *Phys. Chem. Chem. Phys.* **2017**, *19*, 5037-5042.
21. Dubbeldam, D.; Calero, S.; Vlugt, T. J. H.; Krishna, R.; Maesen, T. L. M.; Smit, B., United Atom Force Field for Alkanes in Nanoporous Materials. *J. Phys. Chem. B* **2004**, *108*, 12301-12313.
22. Granato, M. A.; Vlugt, T. J.; Rodrigues, A. E., Molecular Simulation of Propane− Propylene Binary Adsorption Equilibrium in Zeolite 13x. *Ind. Eng. Chem. Res.* **2007**, *46*, 7239-7245.
23. Zhang, Y.; Furukawa, S.-i.; Nitta, T., Molecular Simulation Studies on Adsorption of Propane/Propylene in Naa Zeolite by Using a Monte Carlo Technique. *J. Chem. Eng. Jpn.* **2003**, *36*, 1085-1094.
24. Makowski, W., Quasi-Equilibrated Temperature Programmed Desorption and Adsorption: A New Method for Determination of the Isosteric Adsorption Heat. *Thermochim. Acta* **2007**, *454*, 26-32.
25. Makowski, W.; Ogorzałek, Ł., Determination of the Adsorption Heat of N-Hexane and N-Heptane on Zeolites Beta, L, 5a, 13x, Y and Zsm-5 by Means of Quasi-Equilibrated Temperature-Programmed Desorption and Adsorption (Qe-Tpda). *Thermochim. Acta* **2007**, *465*, 30-39.
26. Sławek, A.; Vicent-Luna, J. M.; Marszałek, B.; Makowski, W.; Calero, S., Ordering of N-Alkanes Adsorbed in the Micropores of Alpo4-5: A Combined Molecular Simulations and Quasi-Equilibrated Thermodesorption Study. *J. Phys. Chem. C* **2017**, *121*, 25292-25302.
27. Peng, D.-Y.; Robinson, D. B., A New Two-Constant Equation of State. *Ind. Eng. Chem. Fundam.* **1976**, *15*, 59-64.
28. Dubbeldam, D.; Torres-Knoop, A.; Walton, K. S., On the Inner Workings of Monte Carlo Codes. *Mol. Simul.* **2013**, *39*, 1253-1292.
29. Dubbeldam, D.; Calero, S.; Ellis, D. E.; Snurr, R. Q., Raspa: Molecular Simulation Software for Adsorption and Diffusion in Flexible Nanoporous Materials. *Mol. Simul.* **2015**, *42*, 81-101.
30. Balestra, S. R. G.; Bueno-Perez, R.; Calero, S., Gaiast. Zenodo, 2016.

31. Iza Database. http://www.iza-structure.org/databases/ (accessed 02/06/2019).
32. Pluth, J. J.; Smith, J. V., Accurate Redetermination of Crystal Structure of Dehydrated Zeolite A. Absence of near Zero Coordination of Sodium. Refinement of Silicon,Aluminum-Ordered Superstructure. *J. Am. Chem. Soc.* **1980**, *102*, 4704-4708.
33. Adams, J.; Haselden, D., The Structure of Dehydrated Zeolite 5a (Sial= 1.02) by Neutron Profile Refinement. *J. Solid State Chem.* **1984**, *51*, 83-90.
34. Barrachin, B.; de Lara, E. C., Determination of the Electric Field in Zeolites Naa, Nacaa and Ca 6 A. Calculation from the Ionic Charge Distribution and Infrared Measurements of the Induced Band of N 2. *Journal of the Chemical Society, Faraday Transactions 2: Molecular and Chemical Physics* **1986**, *82*, 1953-1966.
35. Olson, D. H., The Crystal Structure of Dehydrated Nax. *Zeolites* **1995**, *15*, 439-443.
36. Jang, S. B.; Song, S. H.; Kim, Y., Crystal Structures of Fully Dehydrated Ca^{2+} -Exchanged Zeolite X, Ca_{46}-X, and Ca^{2+} and K^{+}-Exchanged Zeolite X, Ca_{32} K_{28}-X. *Journal of the Korean Chemical Society* **1995**, *39*, 7-13.
37. Engelhardt, G., Cation Location in Dehydrated Zeolite Nay Revisited: Si Position Is Displaced from the Center of the Hexagonal Prism. *Microporous materials* **1997**, *12*, 369-373.
38. Baker, J., An Algorithm for the Location of Transition States. *J. Comput. Chem.* **1986**, *7*, 385-395.
39. Jackson, R.; Catlow, C., Computer Simulation Studies of Zeolite Structure. *Mol. Simul.* **1988**, *1*, 207-224.
40. Sanders, M.; Leslie, M.; Catlow, C., Interatomic Potentials for Sio 2. *J. Chem. Soc., Chem. Commun.* **1984**, 1271-1273.
41. García-Sánchez, A.; García-Pérez, E.; Dubbeldam, D.; Krishna, R.; Calero, S., A Simulation Study of Alkanes in Linde Type a Zeolites. *Adsorpt. Sci. Technol.* **2007**, *25*, 417-427.
42. Liu, B.; Smit, B.; Rey, F.; Valencia, S.; Calero, S., A New United Atom Force Field for Adsorption of Alkenes in Zeolites. *J. Phys. Chem. C* **2008**, *112*, 2492-2498.
43. Zhu, W.; Kapteijn, F.; Moulijn, J.; Den Exter, M.; Jansen, J., Shape Selectivity in Adsorption on the All-Silica Dd3r. *Langmuir* **2000**, *16*, 3322-3329.
44. Olson, D. H.; Camblor, M. A.; Villaescusa, L. A.; Kuehl, G. H., Light Hydrocarbon Sorption Properties of Pure Silica Si-Cha and Itq-3 and High Silica Zsm-58. *Microporous Mesoporous Mater.* **2004**, *67*, 27-33.
45. Palomino, M.; Cantín, A.; Corma, A.; Leiva, S.; Rey, F.; Valencia, S., Pure Silica Itq-32 Zeolite Allows Separation of Linear Olefins from Paraffins. *Chem. Commun.* **2007**, 1233-1235.
46. Narin, G.; Martins, V. F.; Campo, M.; Ribeiro, A. M.; Ferreira, A.; Santos, J. C.; Schumann, K.; Rodrigues, A. E., Light Olefins/Paraffins Separation with 13x Zeolite Binderless Beads. *Sep. Purif. Technol.* **2014**, *133*, 452-475.
47. van Miltenburg, A.; Gascon, J.; Zhu, W.; Kapteijn, F.; Moulijn, J. A., Propylene/Propane Mixture Adsorption on Faujasite Sorbents. *Adsorption* **2008**, *14*, 309-321.
48. Palmas, S.; Polcaro, A. M.; Carta, R.; Tola, G., Sorption and Diffusion of Light Hydrocarbons on Nay Zeolites. *J. Chem. Eng. Data* **1991**, *36*, 1-4.
49. Kresse, G.; Hafner, J., Ab Initio Molecular Dynamics for Liquid Metals. *Phys. Rev. B* **1993**, *47*, 558.
50. Kresse, G.; Hafner, J., Ab Initio Molecular-Dynamics Simulation of the Liquid-Metal–Amorphous-Semiconductor Transition in Germanium. *Phys. Rev. B* **1994**, *49*, 14251.
51. Kresse, G.; Furthmüller, J., Efficiency of Ab-Initio Total Energy Calculations for Metals and Semiconductors Using a Plane-Wave Basis Set. *Comput. Mater. Sci.* **1996**, *6*, 15-50.
52. Kresse, G.; Furthmüller, J., Efficient Iterative Schemes for Ab Initio Total-Energy Calculations Using a Plane-Wave Basis Set. *Phys. Rev. B* **1996**, *54*, 11169.
53. Perdew, J. P.; Burke, K.; Ernzerhof, M., Generalized Gradient Approximation Made Simple. *Phys. Rev. Lett.* **1996**, *77*, 3865.
54. Blöchl, P. E., Projector Augmented-Wave Method. *Phys. Rev. B* **1994**, *50*, 17953.
55. Kresse, G.; Joubert, D., From Ultrasoft Pseudopotentials to the Projector Augmented-Wave Method. *Phys. Rev. B* **1999**, *59*, 1758.
56. Monkhorst, H. J.; Pack, J. D., Special Points for Brillouin-Zone Integrations. *Phys. Rev. B* **1976**, *13*, 5188.
57. Fairen-Jimenez, D.; Galvelis, R.; Torrisi, A.; Gellan, A. D.; Wharmby, M. T.; Wright, P. A.; Mellot-Draznieks, C.; Duren, T., Flexibility and Swing Effect on the Adsorption of Energy-Related Gases on Zif-8: Combined Experimental and Simulation Study. *Dalton Trans.* **2012**, *41*, 10752-10762.
58. Habgood, H., Adsorptive and Gas Chromatographic Properties of Various Cationic Forms of Zeolite X. *Can. J. Chem.* **1964**, *42*, 2340-2350.
59. Yang, R.; Kikkinides, E., New Sorbents for Olefin/Paraffin Separations by Adsorption Via Π-Complexation. *AIChE J.* **1995**, *41*, 509-517.

60. Khelifa, A.; Derriche, Z.; Bengueddach, A., Adsorption of Propene on Nax Zeolite Exchanged with Zn2+ and Cu2+. *Appl. Catal., A* **1999**, *178*, 61-68.
61. Aguado, S.; Bergeret, G. r.; Daniel, C.; Farrusseng, D., Absolute Molecular Sieve Separation of Ethylene/Ethane Mixtures with Silver Zeolite A. *J. Am. Chem. Soc.* **2012**, *134*, 14635-14637.
62. King, C. J., Separation Processes Based on Reversible Chemical Complexation. Wiley: New York: 1987; pp 760-774.
63. Luna-Triguero, A.; Vicent-Luna, J. M.; Becker, T. M.; Vlugt, T. J. H.; Dubbeldam, D.; Gómez-Álvarez, P.; Calero, S., Effective Model for Olefin/Paraffin Separation Using (Co,Fe, Mn, Ni)-Mof-74. *ChemistrySelect* **2017**.
64. Luna-Triguero, A.; Vicent-Luna, J. M.; Gómez-Álvarez, P.; Calero, S., Olefin/Paraffin Separation in Open Metal Site Cu-Btc Metal–Organic Framework. *J. Phys. Chem. C* **2017**, *121*, 3126-3132.
65. Becker, T. M.; Luna-Triguero, A.; Vicent-Luna, J. M.; Lin, L.-C.; Dubbeldam, D.; Calero, S.; Vlugt, T. J., Potential of Polarizable Force Fields for Predicting the Separation Performance of Small Hydrocarbons in M-Mof-74. *Phys. Chem. Chem. Phys.* **2018**, *20*, 28848-28859.
66. Luna-Triguero, A.; Vicent-Luna, J. M.; Poursaeidesfahani, A.; Vlugt, T. J. H.; Sánchez-de-Armas, R.; Gómez-Álvarez, P.; Calero, S., Improving Olefin Purification Using Metal Organic Frameworks with Open Metal Sites. *ACS Applied Materials & Interfaces* **2018**, *10*, 16911-16917.
67. Bloch, E. D.; Queen, W. L.; Krishna, R.; Zadrozny, J. M.; Brown, C. M.; Long, J. R., Hydrocarbon Separations in a Metal-Organic Framework with Open Iron(Ii) Coordination Sites. *Science* **2012**, *335*, 1606-1610.
68. Hampson, J.; Jasra, R.; Rees, L., Sorption of Hydrocarbons in Silicalite-1 and Nay Zeolites. In *Studies in Surface Science and Catalysis*, Elsevier: 1991; Vol. 62, pp 509-517.
69. Divekar, S.; Nanoti, A.; Dasgupta, S.; Chauhan, R.; Gupta, P.; Garg, M. O.; Singh, S. P.; Mishra, I. M., Adsorption Equilibria of Propylene and Propane on Zeolites and Prediction of Their Binary Adsorption with the Ideal Adsorbed Solution Theory. *Journal of Chemical & Engineering Data* **2016**, *61*, 2629-2637.